



**HAL**  
open science

## **Influence of fillers and bonding agents on the viscoelasticity of highly filled elastomers**

Aurélie Azoug, Robert Nevière, Rachel-Marie Pradeilles-Duval, Andrei Constantinescu

► **To cite this version:**

Aurélie Azoug, Robert Nevière, Rachel-Marie Pradeilles-Duval, Andrei Constantinescu. Influence of fillers and bonding agents on the viscoelasticity of highly filled elastomers. *Journal of Applied Polymer Science*, 2014, 131 (16), 10.1002/app.40664 . hal-01219758

**HAL Id: hal-01219758**

**<https://polytechnique.hal.science/hal-01219758v1>**

Submitted on 19 Dec 2022

**HAL** is a multi-disciplinary open access archive for the deposit and dissemination of scientific research documents, whether they are published or not. The documents may come from teaching and research institutions in France or abroad, or from public or private research centers.

L'archive ouverte pluridisciplinaire **HAL**, est destinée au dépôt et à la diffusion de documents scientifiques de niveau recherche, publiés ou non, émanant des établissements d'enseignement et de recherche français ou étrangers, des laboratoires publics ou privés.



Distributed under a Creative Commons Attribution - NonCommercial 4.0 International License

# Influence of Fillers and Bonding Agents on the Viscoelasticity of Highly Filled Elastomers

Aur lie Azoug<sup>1</sup> Robert Nevi re<sup>2</sup> Rachel-Marie Pradeilles-Duval<sup>1</sup> Andrei Constantinescu<sup>1</sup>

<sup>1</sup>Laboratoire de M canique des Solides - CNRS UMR 7649, Ecole Polytechnique, 91128 Palaiseau Cedex, France

<sup>2</sup>SNPE Mat riaux Energetiques, Centre de Recherches du Bouchet, 9 Rue Lavoisier, 91710 Vert-le-Petit, France

**ABSTRACT:** Highly filled elastomers such as solid propellants exhibit a complex nonlinear viscoelastic behavior. This work aimed at determining the influence of binder–filler and filler–filler interactions on the microstructure and the viscoelastic properties of the propellant using a design of experiments method. The influences of the filler fraction and of the filler–binder bonding agents (FBBA) were measured by swelling experiments and prestrained dynamic mechanical analyses. The results showed that FBBA react on the filler surface and concentrate the curing agents in the vicinity of the fillers. The nonlinearity of the viscoelastic behavior originated from filler–filler interactions that created high stress zones between fillers and therefore constrained the movements of the macromolecules of the binder. Filler–binder interactions induced by the FBBA increased the filler effective volume as well as the heterogeneous stress distribution in the microstructure.

**KEYWORDS:** elastomers; mechanical properties; properties and characterization; swelling; viscosity and viscoelasticity

## INTRODUCTION

Solid propellants are highly filled elastomers used for propulsion of rockets and launchers. Their filler volume fraction reaches 80%. Only a small amount of binder holds the particles together and provides viscoelastic properties to the composite up to large strains. The high filler fraction and the physical properties of the filler–binder interaction induce a complex, highly nonlinear mechanical behavior of the composite. Notwithstanding, predictive material models are needed to design the structure of the launchers.

The modeling of the nonlinear viscoelastic mechanical behavior exhibited by highly filled materials is a current research challenge. Phenomenological models<sup>1–5</sup> are inaccurate under multiaxial loadings, whereas homogenization theories<sup>6–9</sup> are only accurate up to a filler fraction of 30%–50%. At high filler fractions, the macroscopic behavior is closely entangled with the physical complexity of the microstructure. At the scale of the polymer chains, macromolecules are either free or cross-linked and interact with plasticizers and the fillers surface. The numerous local mechanisms leading to the measured macroscopic nonlinear behavior make it difficult to distinguish the influence of filler–filler interactions from binder–filler interactions. The peculiar effects of these phenomena on the behavior are neither easy to represent in phenomenological models nor accessible within homogenization theories.

Because of the physical and chemical properties of the binder and the fillers, links are not spontaneously formed between the polymer chains of the binder and the filler surface; the fillers are denoted as nonreinforcing.<sup>10</sup> Consequently, filler–binder bonding agents (FBBA) have to be introduced in the composition to prevent dewetting, i.e., separation between fillers and binder.<sup>11,12</sup> FBBA are low-molecular-weight compounds with several functional groups. Some of the functional groups are reacting with the filler surface, whereas others, such as hydroxyl groups, react with the curing agents of the binder.<sup>12,13</sup> By promoting filler–binder interactions, FBBA have a strong influence on the ultimate strength at large strains,<sup>12</sup> and on the small strain viscoelastic behavior.<sup>10</sup>

Numerous studies have tried to understand and to quantify the influence of the filler fraction on the mechanical behavior of filled elastomers.<sup>14–22</sup> Payne<sup>15</sup> divides the influence of fillers on the nonlinear viscoelastic behavior into three contributions: (a) the hydrodynamic effect, (b) the filler network effect, and (c) the effect of binder–filler linkage. The filler network is defined as “interaggregate association by physical (...) forces.”<sup>17</sup> Similarly, (d) molecular slippage of elastomer chains along the filler surface<sup>18</sup> and (e) geometrical rearrangement of fillers<sup>2</sup> are added to the possible physical mechanisms.

After comparing the sizes and the reinforcing properties of propellant fillers and common carbon black fillers, Stacer et al.<sup>10</sup>

concluded that a filler network does not form in propellants and that the nonlinearity of the viscoelastic behavior is entirely due to the strength of the binder–filler interface. Besides, in conjunction with the binder–filler interactions, the presence of highly packed fillers leads to a highly heterogeneous stress distribution into the microstructure. Numerical simulations of actual filler distributions<sup>9,23,24</sup> show stress localization zones in the binder situated between close adjacent fillers and a difference of an order of magnitude between the global macroscopic and the local microscopic strain.

This work aimed at determining the influence of binder–filler and filler–filler interactions on the propellant microstructure and macroscopic viscoelastic properties, using a large experimental campaign. To differentiate the influence of the fillers from the influence of their interaction with other components, a design of experiment method has been implemented taking into account four factors: the filler fraction, the presence of FBBA, the NCO/OH ratio, and the plasticizer content. The NCO/OH ratio is the ratio of the quantity of curing agents with respect to the quantity of hydroxyl functions in the introduced polymer. In this article, the results quantifying the influence of the first two factors, namely the filler fraction and the presence of FBBA, are discussed. The discussion of the last two factors is presented in an accompanying article.<sup>25</sup>

## EXPERIMENTAL

To comprehend the influence of different factors on the nonlinear behavior as well as to overcome the complexity of the local mechanisms, a D-optimal design of experiments (DoE)<sup>26</sup> was used to program and analyze the experiments. A combination of factors was chosen to span the largest volume within the experimental region in the material parameter space, which created an optimal set of experiments. Four factors defining the material components were chosen in this work: (i) the filler fraction, (ii) the NCO/OH ratio, (iii) the plasticizer content, and (iv) the FBBA. Swelling experiments measured the microscopic parameters, such as the sol polymer fraction and the propellant and binder cross-link densities. The macroscopic viscoelastic behavior was characterized by prestrained dynamic mechanical analyses (PDMA).<sup>27</sup>

### Factors and Materials

The fillers used were ammonium perchlorate and aluminum particles. The size of the ammonium perchlorate fillers lied between 20 and 200  $\mu\text{m}$ , whereas the mean size of the aluminum fillers was 5  $\mu\text{m}$ . The ammonium perchlorate fillers presented a near spherical shape. The shape of the aluminum particles is less regular but is still usually modeled as spherical.<sup>28</sup> For the purpose of determining the deformation mechanisms, all the fillers were considered spherical. The materials must remain highly filled; therefore, the filler fractions of the DoE was varied in mass fraction of  $\pm 2$  wt % around the standard 88 wt % value of the industrial propellant.

The binder was based on hydroxyl-terminated polybutadiene prepolymer cured with a methylene dicyclohexyl isocyanate. The NCO/OH ratio is the ratio of the quantity of isocyanate functions (NCO) with respect to the quantity of hydroxyl

functions (OH). The NCO/OH ratio varied between 0.8 and 1.1. The plasticizer introduced was dioctyl azelate molecules. Plasticizer content lied between 10 and 30 wt % of the binder.

The exact synthesis of the FBBA molecules is confidential and will, therefore, not be described. However, the FBBA are a combination of two molecules, denoted X and Y hereafter.

Molecule X, although reacting with both the ammonium perchlorate filler and the polymeric binder and hence classified as an FBBA, has first been used to increase the ultimate strain of propellants. This molecule reacted with the curing agent and the filler surface. The chemical reaction increased the cross-link density in the vicinity of the fillers and, by consuming curing agents, weakened the polymer network in the binder. This molecule was introduced in each material, independently of the FBBA factor level. Hence, the influence of molecule X on the polymer network was the same for all the materials.

Molecule Y contains aziridine groups that react with the ammonium perchlorate fillers converting the molecule into a polymeric form.<sup>11</sup> This molecule enveloped the filler in a dense strengthening layer.<sup>12,29</sup>

The propellant needs both molecules to create an effective binder–filler adhesion.<sup>30</sup> However, the chemical interactions between the compounds were complex, and the exact mechanisms leading to proper filler–binder adhesion were difficult to quantify. Therefore, this factor was chosen to be categorical and presented two levels: absence (–) or presence (×) of molecule Y.

The materials were thermally cured for 2 weeks at 50°C. Because four factors were chosen, 20 materials were necessary to measure the influence of each factor and their first interaction separately. Two additional materials were manufactured to increase the robustness of the DoE. The levels of the factors for each material are given in Table I.

### Physicochemical Characterization

The swelling experiments followed the swelling to equilibrium procedure.<sup>31</sup> Six specimens for each material were tested. The initial mass of the specimens was  $m_0$ . The specimens were placed in a toluene bath, which was renewed everyday, and their mass was regularly measured. When the mass attained a constant value, swelling equilibrium was reached. The process usually takes 4–5 days.

The specimens were then divided into two groups. Half of the specimens were weighed, and the swollen mass of the propellant  $m_{\text{sp}}$  was obtained. The solvent was then evaporated until a constant dry mass  $m_{\text{dp}}$  was reached. Mass loss  $M_{\text{sf}}$  after extraction and drying indicated the mass of sol fraction in the initial formulation, eq. (1).

$$M_{\text{sf}} = m_0 - m_{\text{dp}} \quad (1)$$

A high quantity of plasticizers was introduced into the premix during manufacturing. Adding these molecules aimed at facilitating the process, particularly the incorporation of fillers, and providing targeted mechanical properties of the final product. Moreover, solid propellants are voluntarily under cross-linked. Consequently, a part of the polymer chains remained unlinked to the network.

Table I. Materials Manufactured Following the DoE Method

Material	Fillers (wt %)	FBBA	NCO/OH ratio	Plasticizer (wt % binder)
0	86	-	1.1	10
1	90	-	0.8	30
2	86	×	1.1	20
3	90	×	0.8	20
4	86	-	1.1	30
5	90	×	1.1	30
6	90	-	0.8	10
7	86	×	0.8	10
8	86	-	0.8	20
9	86	×	0.8	30
10	90	-	0.95	20
11	88	-	1.1	20
12	90	×	1.1	10
13	88	×	0.95	30
14	88	×	0.95	15
15	88	-	0.88	25
16	88	-	0.95	10
17	90	×	0.8	10
18	86	-	0.8	10
19	86	×	1.1	10
20	89	-	1.1	20
21	89	-	0.8	10

Absence or presence of FBBA is denoted by - and ×, respectively.

The sol fraction is defined as the microstructural phase that can be extracted by swelling, meaning the fraction of the binder unlinked to the global polymer network and not contributing to the elastic response. Sol fraction in propellants is mainly constituted of polymer chains and plasticizer molecules. Consequently, the measured mass of sol fraction was the sum of the mass of plasticizer molecules and the mass of sol polymer chains. In the sequel, we shall denote by  $M_{\text{solpol}}$  and  $V_{\text{solpol}}$  the mass and volume of polymer chains in the sol fraction, and by  $M_{\text{plast}}$  and  $V_{\text{plast}}$  the mass and volume of plasticizer molecules.

Extracting a similar propellant with an identical procedure and measuring the quantity of plasticizer molecules in the extracted fraction showed that the quantity of plasticizer in the sol fraction is equal to the quantity introduced during manufacture.<sup>32</sup> This result proves that no link is formed between the plasticizer and the polymer network or the fillers during curing of the polymer. Thus,  $M_{\text{plast}}$  corresponded to the mass of plasticizers introduced during the manufacturing of the material; see Table I. If some additives were extracted, their mass was assumed to be insignificant.  $M_{\text{solpol}}$  was then deduced using eq. (2),

$$M_{\text{solpol}} = M_{\text{sf}} - M_{\text{plast}} \quad (2)$$

The volume of the sol fraction,  $V_{\text{sf}}$ , and of its components were determined using the density of the polymer and the plasticizer,  $\rho_{\text{pol}} = 910 \text{ kg m}^{-3}$  and  $\rho_{\text{plast}} = 920 \text{ kg m}^{-3}$ , respectively.

$$V_{\text{sf}} = V_{\text{solpol}} + V_{\text{plast}} = \frac{M_{\text{solpol}}}{\rho_{\text{pol}}} + \frac{M_{\text{plast}}}{\rho_{\text{plast}}} \quad (3)$$

Finally, the fraction of the sol polymer,  $F_{\text{solpol}}$ , was determined through eq. (4):

$$F_{\text{solpol}} = \frac{V_{\text{solpol}}}{V_{\text{pol}}} = \frac{V_{\text{sf}} - V_{\text{plast}}}{V_{\text{pol}}} \quad (4)$$

where the polymer volume fraction in the binder was  $V_{\text{pol}} = 1 - V_{\text{plast}}$ . Again, the volume of the hydroxyl-terminated polybutadiene polymer chains and the plasticizer molecules was assumed to determine the volume of the binder.

The other half of the specimens was placed in dimethylformamide, which was renewed daily for 5 days, to extract the ammonium perchlorate fillers. Aluminum fillers were not extracted. The swelling to equilibrium procedure in toluene was reiterated. The swollen and dry masses of the binder, denoted  $m_{\text{sb}}$  and  $m_{\text{db}}$ , respectively, were obtained and allowed the determination of the swelling ratios:

$$G_i = \frac{m_{\text{si}}}{m_{\text{di}}} \quad (5)$$

where the subscript  $i$  stands for the propellant,  $p$ , or the binder,  $b$ .

The cross-link densities of the propellant,  $D_p$ , and of the binder,  $D_b$ , defined as moles of cross-links per unit volume, were deduced from the equilibrium swelling ratios according to eq. (6).

$$D_i = -\frac{\ln(1 - V_{2i}) + V_{2i} + \chi_{12} V_{2i}^2}{V_1(V_{2i}^{1/3} - V_{2i}/2)V_0^{2/3}} \quad (6)$$

where the subscript  $i$  stands for either the propellant  $p$  or the binder  $b$  as before,  $V_0$  is the volume fraction of the polymer as cross-linking occurred (here  $V_0=1$ ),  $V_1$  is the molar volume of the solvent,  $V_{2i}$  is the volume fraction of the polymer in the swollen gel fraction and was determined by eq. (7).  $\chi_{12}$  is the Flory–Huggins polymer–solvent interaction parameter equal to 0.355.<sup>33</sup>  $\rho_1$  and  $\rho_2$  are the volume masses of the solvent and the polymer,  $\rho_1 = 0.8869 \text{ g cm}^{-3}$  and  $\rho_2 = 0.9 \text{ g cm}^{-3}$ , respectively.

$$V_{2i} = \frac{1}{1 + G_i \frac{\rho_2}{\rho_1}} \quad (7)$$

$F_{\text{solpol}}$ ,  $D_p$ , and  $D_b$  constituted three DoE responses characterizing the microstructure and were analyzed according to the procedure described in the DoE Analysis Section.

### Prestrained Dynamic Mechanical Analysis

The PDMA procedure used in this study superimposed a tensile prestrain on small strain oscillations, which allowed the measurement of the nonlinear viscoelastic behavior at large strains. This procedure has been previously discussed.<sup>27,34,35</sup>

PDMA experiments were achieved using a Metravib Viscoanalyseur VA3000. Rectangular specimens of dimension 50 mm × 10 mm × 5 mm were used. The experimental procedure consisted of superimposing a tensile prestrain to a tensile sinusoidal strain onto the specimen, which defined a total strain of:

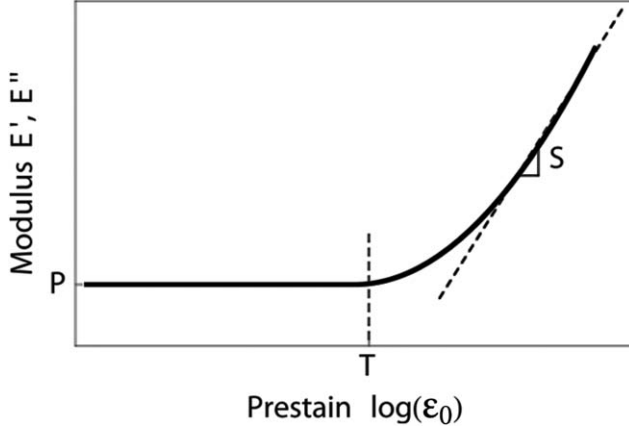


Figure 1. Schematic representation of the quantification of the viscoelastic behavior.

$$\varepsilon(t) = \varepsilon_0 + \varepsilon_a \sin(2\pi ft) \quad (8)$$

where the strain amplitude is  $\varepsilon_a = 0.01\%$ ,  $0.1\%$ , or  $0.5\%$ , and the frequency is  $f = 5$  Hz. The tests were performed at room temperature. Different levels of prestrain  $\varepsilon_{0,i}$  were reached from  $0.01\%$  to about  $10\%$ .<sup>34</sup>

The norm of the complex modulus  $\|E^*\|$  and the loss factor  $\tan \delta$  were determined at each prestrain level. The storage and loss moduli,  $E'$  and  $E''$ , were deduced from these values using:

$$\|E^*\| = \sqrt{E'^2 + E''^2} \quad \text{and} \quad \tan \delta = \frac{E''}{E'} \quad (9)$$

The storage modulus,  $E'$ , quantifies the elastic part of the behavior whereas the loss modulus,  $E''$ , corresponds to the quantity of heat dissipated by friction between polymer chains during a strain cycle.<sup>16</sup> Assuming that the material behavior can be represented by a linear rheological model,  $E''$  is also directly linked to the viscosity of the composite.

To quantify the variation of  $E'$  and  $E''$ , we shall use the phenomenological model proposed in previous articles.<sup>27,35</sup> It has been shown that the behavior can be decomposed into a linear domain and a nonlinear domain (Figure 1). If  $M$  stands for the storage modulus  $E'$  or the loss modulus  $E''$ , a unique model, eq. (10), was used to approximate both curves. The constants  $\alpha$ ,  $\beta$ ,  $\varepsilon_p$ ,  $\gamma$ , and  $\xi$  were identified from the experimental results using a least-squares optimization algorithm in Mathematica®.

$$M = \begin{cases} \alpha + \beta \log \varepsilon_0 & \varepsilon_0 < \varepsilon_p \\ \alpha + \beta \log \varepsilon_0 + \gamma \left[ \log \left( \frac{\varepsilon_0}{\varepsilon_p} \right) \right]^\xi & \text{else.} \end{cases} \quad (10)$$

The responses of a DoE have to be numerical quantity that can be systematically determined for each material and then statistically analyzed. The viscoelastic behavior of the material according to prestrain was quantified by three parameters that characterize each domain and the threshold between them (Figure 1). The plateau value  $P$  characterizes the linear domain and is the model response at the chosen value  $\varepsilon_0 = \varepsilon_p$ , see eq. (11).

$$P = \alpha + \beta \log \varepsilon_p \quad (11)$$

where  $\varepsilon_p = 0.01\%$ .

The nonlinearity threshold  $T$  is directly given by  $\varepsilon_p$ . The nonlinearity domain is characterized by its slope  $S$ , which is the mean value of  $N$  tangents to the curve at  $\varepsilon_0$  higher than  $\varepsilon_p$  [eq. (12)].

$$S = \frac{1}{N} \sum_{i=1}^N \left\{ \beta + \gamma \xi \left[ \log \left( \frac{\varepsilon_t + \varepsilon_i}{\varepsilon_t} \right) \right]^{\xi-1} \right\} \quad (12)$$

where  $\varepsilon_i \in [3\%, 6\%]$  and  $N = 16$  is the chosen number of tangents.

In the following sections, superscripts  $(\bullet)'$  and  $(\bullet)''$  were added to the parameters to denote the application for the storage modulus  $E'$  or the loss modulus  $E''$ , respectively. The macroscopic viscoelastic behavior of each material, quantified by  $P$ ,  $T$ , and  $S$ , was analyzed according to the procedure described in the next section.

### Analysis of the DoE Responses

Using the Design-Expert® software,<sup>36</sup> the analysis of the response was performed in the classical frame of design of experiments.<sup>37</sup> The responses  $R$  of the materials were the results of the experimental procedures described in the previous sections, i.e.,  $F_{\text{sol/pol}}$ ,  $D_p$ ,  $D_b$ ,  $P$ ,  $T$ , and  $S$ .

A model with  $n$  coefficients can only be investigated with a DoE consisting of at least  $n$  runs. According to the number of factors chosen and the number of materials manufactured, the possible models were:

- Mean value:  $R = m$
- Linear:  $R = m + \sum_{i=1}^4 c_i F_i$
- First-order interactions:  $R = m + \sum_{\substack{i,j=1 \\ i < j}}^4 (c_i F_i + d_{ij} F_i F_j)$
- Quadratic:  $R = m + \sum_{\substack{i,j=1 \\ i < j}}^4 (c_i F_i + e_i F_i^2 + d_{ij} F_i F_j)$

where  $R$  is the response for the material depending on the factors  $F = \{F_1, \dots, F_n\}$ ,  $m$  stands for the mean value of the response, and the unknowns  $c_i$ ,  $d_{ij}$ , and  $e_i$  were obtained by optimization on the experimental results. An analysis of variance determined the model form best representing the results while taking into account the least number of terms. A second analysis of variance was performed on the chosen model form to eliminate the terms corresponding to noninfluential factors or interactions ( $p$ -value  $< 0.05$ ). Any necessary transformation of the data was determined by a Box-Cox plot,<sup>38</sup> and the analysis was then repeated with the transformed data.

The final model represented the response according to the factors of the DoE, here variables of material composition. The good fit of the model was evaluated by the adjusted correlation coefficient  $R_{\text{adj}}^2$ , which took into account the number of terms in the model.<sup>39</sup>

## RESULTS AND DISCUSSION

The fit of the models with respect to the experimental data is discussed in the second part of this study.<sup>25</sup> The results discussed next show the influence of the filler fraction and the presence of FBBA on the microstructure and the viscoelastic behavior.

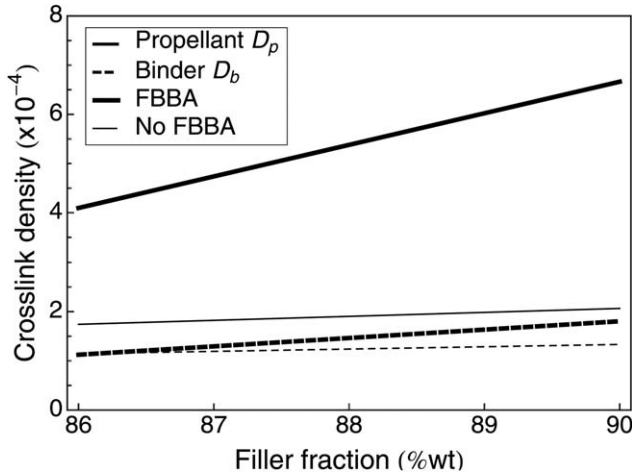


Figure 2. Influence of filler fraction and FBBA on the cross-link density of the propellant  $D_p$  and of the binder  $D_b$ . NCO/OH = 0.95, plasticizer = 20 wt % of the binder.

### Microstructure

As a first outcome to the analysis, we can state that increasing the filler fraction leads to an increase in the cross-link density of the propellant  $D_p$  and of the binder  $D_b$ . Figure 2 represents the influence of the interaction between FBBA and filler fraction on the cross-link densities. When FBBA are present, an increase in filler fraction lead to a strong increase in cross-link densities  $D_p$  and  $D_b$ . In the absence of FBBA, the filler fraction had a weak influence on the cross-link densities.

The increase in propellant cross-link density  $D_p$  with filler fraction confirmed that FBBA were indeed creating links between the filler surface and the binder. A strong interaction between the two factors was expected as FBBA are chemically activated by the fillers. It also confirmed that both molecule X and molecule Y were necessary to promote filler–binder adhesion. Molecule X did not produce an effective adhesion between fillers and binder<sup>25</sup> because the cross-link density did not depend on the filler fraction in the materials containing no FBBA, that is, where the molecule Y was absent.

The binder cross-link density  $D_b$  depended unexpectedly on filler fraction when molecule Y was added. The aziridine cycles in molecule Y homopolymerized around the ammonium perchlorate fillers. This reaction created a strong polymer layer around the filler that will not be dissolved with the filler. As a consequence,  $D_b$  still increased with filler fraction even though the fillers were removed from the microstructure. Therefore,  $D_b$  was not an exact measurement of the binder cross-link density, from which the influence of filler–binder adhesion would have been eliminated. Because  $D_b$  depended on the filler fraction, it seemed that a significant fraction of the cross-links was situated on the filler surface when FBBA were introduced.

The sol polymer fraction  $F_{solpol}$  increased linearly with filler fraction and decreased when FBBA were added (Figure 3).

At first glance, the increase in the sol polymer fraction with the filler fraction seemed inconsistent with the increase in cross-link density in the presence of FBBA. This can be explained by

observing the action of molecule X. As this molecule reacted with the fillers, it blocked the curing agents, and thus they will not be available for building the polymer network. The cross-link density increased around the filler whereas the actual cross-link density of the polymer network was assumed to decrease in the bulk of the binder. The molecule X created an imbalance of curing agents distribution, and, hence, a gradient of cross-link density into the microstructure. The fraction of polymer chains linked to the network decreased whereas the sol polymer fraction increased.

It should be noticed that the cross-link density of material 1 could not be measured. As the material was placed in the solvent, the sol polymer fraction was so large that the material dissolved and fillers were also extracted. Although this material contained 90 wt % of fillers, the NCO/OH ratio was low, and the plasticizer content was high. The links created by molecule X between the fillers and the polymer chains deprived the binder network of too many curing agents, and the global network did not provide enough binding to create a solid material. Hence, when no FBBA were added, the cross-link density of the binder was only lightly influenced by the filler fraction whereas the quantity of sol polymer can increase strongly until a global network no longer exists.

The FBBA reacted with polymer chains in the network or in the sol fraction alike. Therefore, at a constant amount of curing agents, the increase in FBBA will directly decrease the sol polymer fraction.

### Macroscopic Behavior

The plateau values  $P$  and  $P'$  increased almost linearly with the filler fraction (Figures 4 and 5). An effect of the filler fraction was a decrease in the total quantity of polymer per unit volume and therefore increased hydrodynamic and strain amplification effects.<sup>40</sup> This was also due to the high filler fraction of propellant materials where fillers can be considered as rigid and where the polymer network was constrained between the neighboring fillers.

Another effect of the increase in filler fraction is an increase in sol polymer fraction. The sol polymer was considered to move freely within the microstructure and did not directly influence

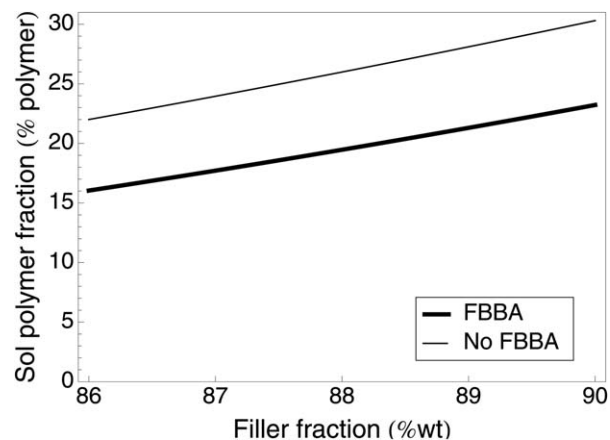


Figure 3. Influence of filler fraction and FBBA on the sol polymer fraction  $F_{solpol}$ . NCO/OH = 0.95, plasticizer = 20 wt % of the binder.

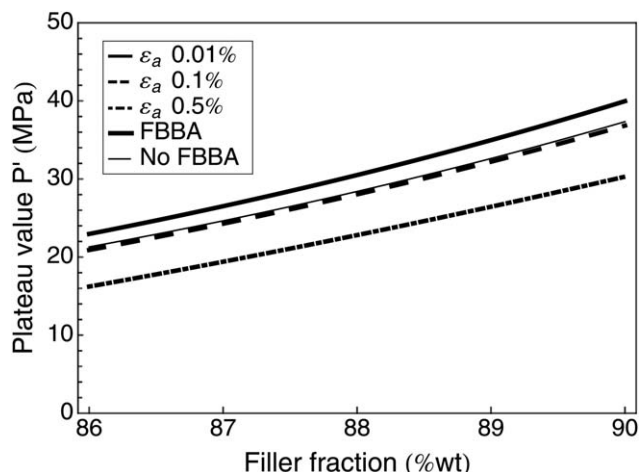


Figure 4. Influence of filler fraction and FBBA on the plateau value  $P'$ . NCO/OH = 0.95, plasticizer = 20 wt % of the binder.

the elastic branch of the composite. However, the movement generated a considerable amount of intermolecular friction, which was translated into a viscous effect. We can resume by saying that as dissipation increases  $P''$  increases.

Figures 4 and 5 show that the plateau values  $P'$  and  $P''$  decreased when the strain amplitude increased. This effect, often called Payne effect, is generally attributed to the destruction of the filler structure in elastomers filled with reinforcing fillers such as carbon black.<sup>15,16</sup> For highly filled elastomers, the fillers introduced are nonreinforcing and do not form agglomerates, and one cannot assume the existence of a filler structure. However, increasing the amplitude of the strain oscillations is favorable to microstructural movements. The polymer chains position around the fillers was modified, which limited the constraint imposed by such a high filler fraction on the polymer network. At this point, the filler geometrical arrangement was assumed to disturb the deformation of the polymer network in response to the imposed loading.

The plateau value  $P'$  of the storage modulus increased with the presence of FBBA at low strain amplitude (Figure 4). This factor had no influence at high amplitudes.

Although the measured sol fraction and cross-link densities depend on FBBA (see the discussion of the microstructure), the influence of this factor on  $P'$  was limited. Two effects of the presence of FBBA were combined on the response  $P'$ . First, as the polymer network is linked to the fillers by the FBBA chemical reaction, the fillers acting as giant cross-links disturb the strain distribution in the binder. Therefore, the FBBA molecules intensified the influence of fillers on the behavior and increased the plateau value  $P'$  of the storage modulus. Second, adding FBBA concentrated the cross-links around the fillers and deprived the network of curing agents. Decrease in the cross-link density of the polymer network inevitably lead to a decrease in storage modulus  $P'$ .

The loss modulus plateau values  $P''$  increased with FBBA at all amplitudes, although the influence of FBBA was reduced with increasing strain amplitude (Figure 5).

The FBBA reacted chemically with the filler surface, curing agents, and polymer chains. They created a reinforcing layer of

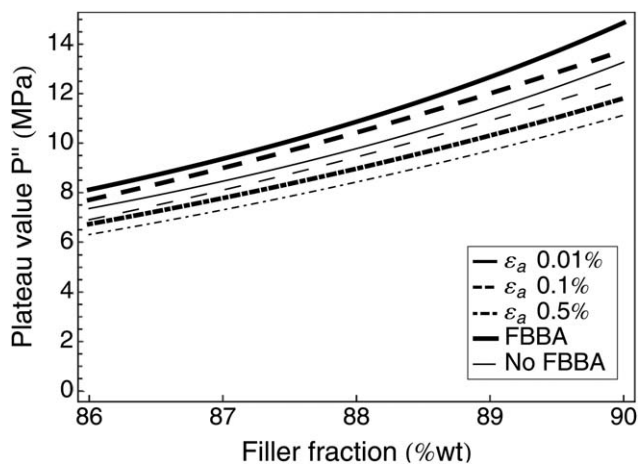


Figure 5. Influence of filler fraction and FBBA on the plateau value  $P''$ . NCO/OH = 0.95, plasticizer = 20 wt % of the binder.

high modulus polymer around the filler. This layer increased the effective volume of the fillers and linked the polymer network to the surface of the fillers. The constraints imposed on the polymer network were then strongly amplified and dissipations in the microstructure increased. As already discussed, the constraints imposed by the fillers on the polymer network were partially released by an increase in strain amplitude.

The filler fraction had the expected influence on the threshold values  $T'$  for  $\epsilon_a = 0.01\%$  and  $T''$  for both amplitudes, i.e., the threshold decreased as the filler fraction increased (Figures 6 and 7). Moreover, the threshold values increased with increasing strain amplitude.

A similar increase in storage and loss modulus with prestrain was observed on filled elastomers at higher prestrains. It was associated with the limit of the extensibility of the network.<sup>41</sup> As already remarked, the high filler fraction induced strain amplification at the microscopic level, which translated into a decrease in the macroscopically measured threshold.

Contrary to expectations, the threshold  $T'$  for a strain amplitude of 0.1% did not depend on the filler fraction. This lack of

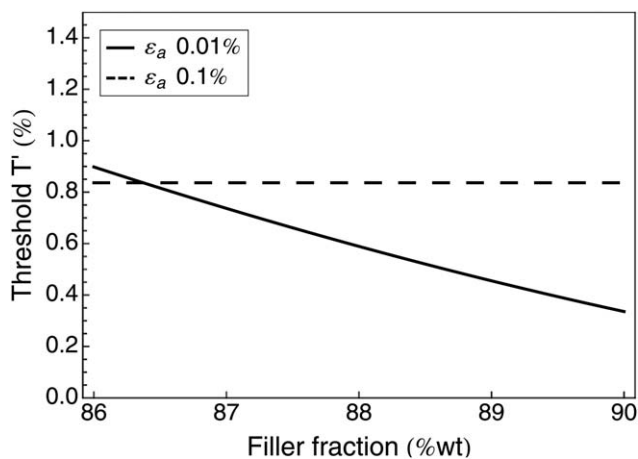


Figure 6. Influence of the filler fraction on the storage modulus threshold  $T'$ . NCO/OH = 0.95, plasticizer = 20 wt % of the binder.

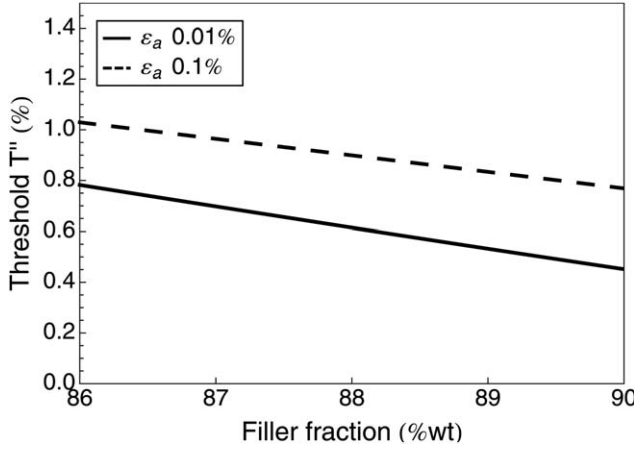


Figure 7. Influence of the filler fraction on the loss modulus threshold  $T''$ . NCO/OH = 0.95, plasticizer = 20 wt % of the binder.

influence was attributed to two causes. First, as previously stated,<sup>27,35</sup> the determination of the threshold was a weak point of the model. Second, the DoE maximized the information from a chosen number of materials but did not guarantee that the information can be obtained in whole. As a consequence, the data might still be insufficient to clearly differentiate the influence of all the factors, especially in scattered responses. Therefore, the sensitivity of the threshold  $T$  was not robust enough to advance further discussion of the deformation mechanism.

The filler fraction was the most influential factor on the nonlinearity slopes  $S'$  and  $S''$  for every strain amplitudes  $\epsilon_a$  (Figures 8 and 9). Although all  $S$  increased with increasing filler fraction, the influence of filler fraction on  $S$  was highly dependent on the strain amplitude  $\epsilon_a$ . Moreover, the influence of filler fraction on the slopes was linear at high strain amplitude, whereas it was nonlinear at low strain amplitude.

The increase in the slopes  $S'$  and  $S''$  with filler fraction was directly linked to the strain amplification by the fillers. More-

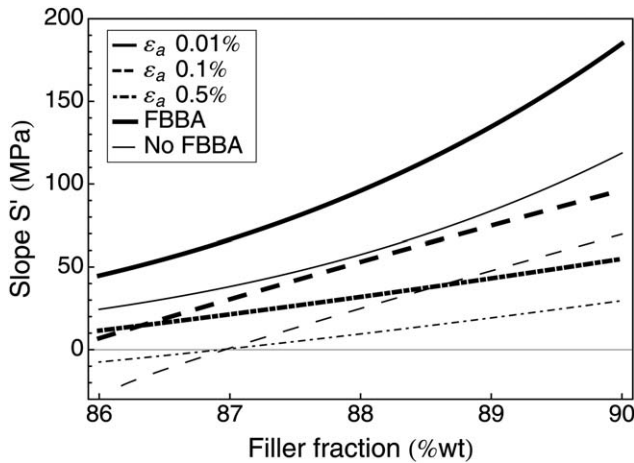


Figure 8. Influence of the filler fraction and FBBA on the nonlinearity slope  $S'$ ; NCO/OH ratio = 0.95, plasticizer = 20 wt % of the binder.

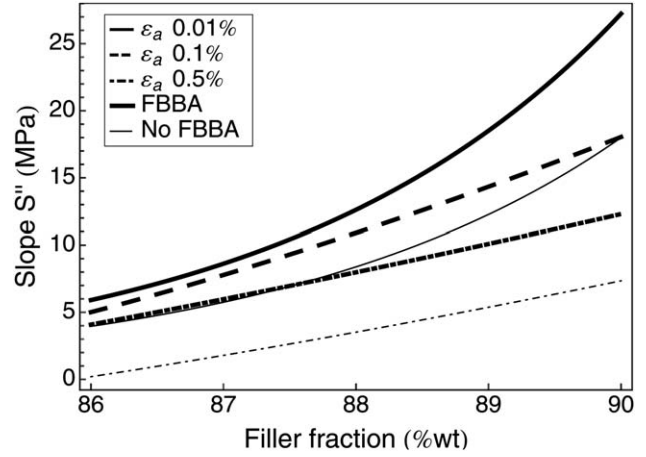


Figure 9. Influence of the filler fraction and FBBA on the nonlinearity slope  $S''$ ; NCO/OH ratio = 0.95, plasticizer = 20 wt % of the binder.

over, the significant influence of the strain amplitude and the nonlinear influence of the filler fraction for low strain amplitudes suggested that another mechanism also occurred. We suggest that, in highly filled elastomers, the observed mechanical behavior is related to the aligning of the solid filler particles according to the applied strain direction.

In highly filled systems like solid propellants, stress concentrations appeared between adjacent close particles, depending on their size.<sup>9</sup> In addition, bands of increased stress were created, as those particles align in the direction of the applied strain.<sup>24</sup> The polymer network between those particles was highly strained and reached its finite extensibility at lower prestrain than the rest of the binder. The nonlinear domain corresponded to the state where the fillers align in the direction of the prestrain and reached a “locked” state, imposing severe restrictions on the polymer chains. As the prestrain increased in the nonlinear domain, the blocked fraction of the binder increased.

Following this hypothesis, the increase in the strain amplitude lowered the constraints imposed by the fillers on the polymer chains and the blocked portions of the network were then released. Consequently, the slope of the storage modulus  $S'$  decreased. As the released polymer chains recaptured mobility, the dissipation decreased. Therefore, we observed a reduction in  $S''$  with increasing prestrain. On the other hand, when the strain amplitude was low, the fraction of fillers in a locked state increased nonlinearly, and the microstructural movements were not large enough to relieve these constraints.

The slopes  $S'$  and  $S''$  increased in the presence of FBBA at all the measured strain amplitudes (Figures 8 and 9). The slopes were linked to a physical mechanism involving filler alignment in the prestrain direction. This mechanism created high stress bands and constrained the polymer chains. Because adding FBBA linked the polymer network to the filler surface and increased the filler effective volume, it directly affected the constraints imposed by the fillers on the polymer chains. As a consequence, all slopes increased with FBBA.

## CONCLUSIONS

We studied the influence of binder–filler and filler–filler interactions on the microstructure and viscoelastic behavior of a solid propellant similar to the industrial composition and containing reactive fillers. Thus, the influence of additives such as FBBA was measured without any assumption. We programmed and analyzed a series of experiments on a large basis of materials using a design of experiments that took into account four factors: the filler fraction, the presence of FBBA, the NCO/OH ratio, and the plasticizer content.

This article presents the influence of the fillers and their interaction with the binder, i.e., the influence of the filler fraction and FBBA factors. The results concerning the influence of the binder (NCO/OH ratio and plasticizer content) will be discussed in an accompanying article.<sup>25</sup>

The microstructure of the materials was characterized by swelling experiments. The sol polymer fraction and the cross-link density of the propellant and the binder were deduced. The nonlinear viscoelastic behavior was determined by PDMA tests. Using a phenomenological model, the nonlinearity of each material was quantified and processed in the classical frame of design of experiments.

The fillers alone did not have a strong influence on the microstructure. However, the added FBBA reacted on the surface of the fillers and created an imbalance of cross-links, concentrating the curing agents in the vicinity of the fillers. Consequently, the quantity of fillers modified the formed polymer network.

The fillers had a strong influence on the viscoelastic measurements. Apart from expected hydrodynamic and strain amplification effects, filler–filler interactions created high-stress zones between adjacent fillers and constrained the polymeric network. Fillers geometrical rearrangement according to prestrain could lead to a locked situation corresponding to the observed nonlinear domain. In addition, filler–binder interactions promoted by the FBBA amplified this effect by increasing the filler effective volume and the heterogeneous stress distribution into the microstructure.

The goal of this study was to widely explore the influence of the composition on the mechanical behavior of highly filled elastomers. Future works should focus on detailing the chemical interaction between the constituents, especially the interaction between the fillers and the plasticizer molecules through the action of the FBBA. A targeted mixture design of experiments can provide answers regarding these mechanisms.

## ACKNOWLEDGMENTS

The work of A.A. is financially supported by DGA, Délégation Générale pour l'Armement (France). The authors thank Mrs. Amiet (DGA) for supporting this project.

## REFERENCES

1. Schapery, R. A. *Eng. Fract. Mech.* **1986**, *25*, 845.
2. Ozupek, S.; Becker, E. B. *J. Eng. Mater. Technol.* **1992**, *114*, 111.
3. Ozupek, S.; Becker, E. B. *J. Eng. Mater. Technol.* **1997**, *119*, 125.
4. Ravichandran, G.; Liu, C. T. *Int. J. Solids Struct.* **1995**, *32*, 979.
5. Jung, G. D.; Youn, S. K.; Kim, B. K. *Int. J. Solids Struct.* **2000**, *37*, 4715.
6. Nadot-Martin, C.; Trumel, H.; Dragon, A. *Eur. J. Mech. A: Solids* **2003**, *22*, 89.
7. Dartois, S.; Halm, D.; Nadot, C.; Dragon, A.; Fanget, A. *Eng. Fract. Mech.* **2008**, *75*, 3428.
8. Xu, F.; Aravas, N.; Sofronis, P. *J. Mech. Phys. Solids* **2008**, *56*, 2050.
9. Matouš, K.; Inglis, H.; Gu, X.; Ryppl, D.; Jackson, T.; Geubelle, P. *Compos. Sci. Technol.* **2007**, *67*, 1694.
10. Stacer, R. G.; Hubner, C.; Husband, D. M. *Rubber Chem. Technol.* **1990**, *63*, 488.
11. Davenas, A. In *Technologie des Propergols Solides*; Davenas, A., Ed.; Masson: Paris, **1989**; Chapter 10.
12. Oberth, A. E.; Bruenner, R. S. In *Propellants Manufacture, Hazards, and Testing*; Gould, R. F., Ed.; Advances in Chemistry Series 88; American Chemical Society: New York, **1969**; pp 84–121.
13. Nema, S. K.; Nair, P. R.; Francis, A. U.; Gowariker, V. R. Presented at Proceedings of the AIAA/SAE 13th Propulsion Conference, Orlando, FL, USA, July 11–13, **1977**.
14. Guth, E. *J. Appl. Phys.* **1945**, *16*, 20.
15. Payne, A. R. *J. Appl. Polym. Sci.* **1962**, *6*, 368.
16. Kraus, G. *Angew. Makromol. Chem.* **1977**, *60*, 215.
17. Medalia, A. I. *Rubber Chem. Technol.* **1978**, *51*, 437.
18. Voet, A. *J. Polym. Sci. Macromol. Rev.* **1980**, *15*, 327.
19. Wang, M. *J. Rubber Chem. Technol.* **1998**, *71*, 520.
20. Leblanc, J. L. *J. Appl. Polym. Sci.* **2000**, *78*, 1541.
21. Heinrich, G.; Kluppel, M.; Vilgis, T. A. *Curr. Opin. Solid State Mater. Sci.* **2002**, *6*, 195.
22. Fukahori, Y. *Rubber Chem. Technol.* **2007**, *80*, 701.
23. Inglis, H. M.; Geubelle, P. H.; Matouš, K. *Philos. Mag.* **2008**, *88*, 2373.
24. Azoug, A. *Micromécanismes et comportement macroscopique d'un élastomère fortement chargé*. Ph.D. Thesis; Ecole Polytechnique: Palaiseau, France, October **2010**.
25. Azoug, A.; Nevière, R.; Pradeilles-Duval, R. M.; Constantinescu, A. *J. Appl. Polym. Sci.* **2014**, DOI: 10.1002/app.40392.
26. Fedorov, V. *Theory of Optimal Experiments*. Academic Press: New York, **1972**.
27. Azoug, A.; Constantinescu, A.; Pradeilles-Duval, R. M.; Vallat, M. F.; Nevière, R.; Haidar, B. *J. Appl. Polym. Sci.* **2013**, *127*, 1772.
28. Gallier, S.; Hiernard F. *J. Propul. Power* **2008**, *24*, 154.
29. Gercel, B. O.; Üner, D. O.; Pekel, F.; Özkar, S. *J. Appl. Polym. Sci.* **2001**, *80*, 806.
30. Kolodziej, M. Master Thesis. Formation d'ingénieurs de l'Université Paris Sud, Orsay, France, **2010**.
31. Flory, P.; Rehner, J. *J. Chem. Phys.* **1943**, *11*, 521.

32. Desgardin, N.; Chevalier, S.; Grevin, M. *Duree de vie, Technical Report CRB N\_ 12/06/CRB/DPS/CRA/DR*, **2006**.
33. Jain, S.; Sekkar, V.; Krishnamurthy, V. *J. Appl. Polym. Sci.* **1993**, *48*, 1515.
34. Thorin, A.; Azoug, A.; Constantinescu, A. *Polym. Test.* **2012**, *31*, 978.
35. Azoug, A.; Thorin, A.; Nevier, R.; Pradeilles-Duval, R. M.; Constantinescu, A. *Polym. Test.* **2013**, *32*, 375.
36. Stat-Ease Software. Available at: <http://www.statease.com/software.html>.
37. Mead, R. *The Design of Experiments: Statistical Principles for Practical Applications*; Cambridge University Press: Cambridge, **1988**.
38. Box, G.; Cox, D. *J. R. Stat. Soc. Series B Stat. Methodol.* **1964**, *26*, 211.
39. Ezekiel, M. *J. Am. Stat. Assoc.* **1929**, *24*, 99.
40. Mullins, L.; Tobin, N. *J. Appl. Polym. Sci.* **1965**, *9*, 2993.
41. Voet, A.; Morawski, J. C. *Rubber Chem. Technol.* **1974**, *47*, 765.